Monitoring and Quantifying Burn Wounds on Pig Skin using Thermal Measurements

Abdusalam Al-khwaji
AL Asmarya Islamic University, Zliten, Libya
Email : a.alkhwaji@asmarya.edu.ly

Tom Diller
Virginia Tech, Blacksburg, USA
Email : tdiller@vt.edu

Abstract—**A new thermal method for detecting burn severity or monitoring burn wound healing is presented. The thermal measurement method avoids the need for introducing any substance or radiation to monitor blood perfusion or detect the depth of burnt tissue. The method of predicting and monitoring burns was tested experimentally by implementing four different burn severities on two pigs and monitoring the burns over five days. Averaged estimated thermal resistance and blood perfusion values were used to detect burn depth from thermal measurements. A damage function was introduced to illustrate those burns which cause third degree burns. The 20 and 75-second burns were quantified as third degree burns. The laboratory measured non-perfused layers calibrates very well with the estimated burn depth from the perfusion-thermal resistance probe. This paper has demonstrated the ability of perfusion-thermal resistance probe to characterize burn severity.**

*Index Term*s*:* **burn depth; bioheat; parameter estimation; thermal measurement; heat flux sensor.**

I. INTRODUCTION

Treating burn wounds requires sufficient knowledge about the burn severity. A burn wound is categorized as first, superficial second, deep second or third degree [5]. The healing process is reported to be between 14 to 21 days after which an excision and grafting surgery is required [5]. A false prediction of the burn depth causes needless surgery or increased hospital accommodation costs [5]. This brings an additional medical significance to this work to decrease the time required to detect the need of surgery.

Burn assessment researchers have developed many invasive and non-invasive techniques to detect burn depths. Invasive techniques are accompanied with either pain or risk of bacterial infection. VACUETTE [19] venous blood sampling device is an invasive device that uses blood perfusion samples to detect burns. Non-invasive techniques range from visual inspection to the use of any of the existing imaging techniques such as thermography (IR), ultrasonography (USG), laser Doppler imaging (LDI) and indocyanine green fluorescence (ICG) [6].

However, none of these techniques has been broadly accepted as a standard diagnostic tool for burns [6]. Non-invasive medical diagnostic methods to predict burn depths are designed to use either information about temperature distribution or the presence of blood perfusion in the burnt area [5-10]. Non-invasive methods such as, radioactive isotopes, or indocyanine green fluorescence (ICG) requires injecting the patient intravenously with radioactive phosphorus [5, 20]. The process requires repeatedly imaging the uptake and clearance of the dye-marker from the burnt region [20]. The vital dye substance such as tetracycline illuminates the burnt area with ultraviolet light, which helps to detect the presence of the dye at specific depths [5]. Thermography or IR thermal imaging techniques are either static or dynamic. In the static IR method, temperature measurements cannot reflect perfusion because it is operating at steady state [5, 6], while the dynamic method involves introducing a thermal event (external thermal excitation) followed by measurements of transient temperature on the burnt surface. The temperature distribution from the dynamic IR method helps to create an image which describes blood perfusion in the burnt area [6]. IR methods are still under research and blood perfusion values are not connected to heat flux from the burnt surface. LDI methods operates on the principle that laser light reflected by the skin undergoes a frequency shift that is correlated by the movement of red cells [21].

Detecting the histology of a burn using any of the imaging techniques beside, Ultrasound and laser Doppler Imaging are expensive and have risks of developing cancer, since pre-injured regions are more common to receive mutation. Most of the imaging techniques collect data to map blood perfusion distribution through a burnt tissue. Only LDI [8] can characterize burns closer to the surface, other imaging techniques detect perfusion in deeper layers only.

Penetration of the used energy waveform reflects the burn depth. The strength of the reflected portion of the energy source indicates sophisticate information about blood perfusion [5-10]. Imaging methods are accomplished with receiving the reflected energy after the attenuation made by blood perfusion and different tissue layers. Using additional substance to either defuse through burnt region or penetrating energy with specific wavelength to defuse through damaged tissue might disturb the healing process. There are no quantification and calibrating results from imaging measurements or the vital dye method, they have risk factor and require extra clinical judgment.

The usage of heat flux measurements in burn assessments is a new method to diagnose a burnt area, where blood perfusion information could be estimated from the perfusion probe [15-17]. Since burn degree effects perfusion which results in changes in temperature and heat transfer through burnt tissue. Using thermal measurement, we built an analytical model, which uses thermal measurements to monitor and detect burnt area. In our previous publication[1-2], we proved the sensitivity and repeatability of the thermal measurements using perfusion-thermal resistance probe "phantom tissue" in characterizing simulated burns, the model was successfully able to classify thicknesses and thermal properties of different layers of Kapton and Lexan [2]. Transportation of heat and perfusion were modeled mathematically using 1D bioheat equation by thermal resistance and blood perfusion.

This work is to quantify different burns on two pigs. The hypotheses of this experiment are to detect the third degree burn from four different burn times, to connect blood perfusion and thermal resistance of the burnt tissue to better illustrate the healing direction, and to minimize the diagnostic time of self-healing.

II. EXPERIMENTAL METHOD

The general study design of this project is a common one used for evaluation of burn injury and has frequently been used for studies in our laboratory. Swine are used since their skin is similar to humans. By exposing the animals skin to brass cylinders of known temperature for a given time period, the depth of burn may be controlled. Four different depths of burn will be evaluated to determine the ability of the different devices to evaluate burn depth and to determine whether it is better than clinical evaluation to predict an endpoint of healing at two weeks.

Eight areas for wounds will be drawn on each side of the anesthetized animal (8 total wounds per pig and 8 control sites) that measure approximately 3 cm diameter. Marked sites will be assigned to one of four treatment groups (i.e. two test groups per animal) or as a control adjacent to the burn site with an intervening 4 cm gap of normal skin. Wounds will be made in the marked areas with a brass cylinder heated to 100 degrees Centigrade. Four different contact times will allow for four different depths of wounds.   Contact times will be 3 seconds, (superficial partial thickness), 12 second (intermediate partial thickness), 20 second deep partial thickness, and 75 second (full thickness). Within the first 10 minutes after injuring, standardized digital photos, B-mode high resolution ultrasonography, heat flux blood perfusion, scanning laser doppler and Periodic camera photos will be obtained. All measurements will be repeated at 1 hour and at 24, 72, and 120 hours. Subsequent photographic evaluations will only be obtained at 7 days and 14 days. Each wound will be covered with Acticoat® (Westaim Laboratories, Edmonton, Alberta) dressing material and an occlusive dressing placed on top. The pigs will then be wrapped to prevent the dressings from falling or being rubbed off by the animal using a technique previously developed in our lab. The animals will be examined once daily for overall condition. Dressings will be changed with each early evaluation or when standardized digital photos are obtained. At 2 weeks, animals will be euthanized by lethal overdose with pentobarbital after collecting the last final data point.

III. MEASUREMENT METHOD & MATHEMATICAL MODEL

A combined heat flux and temperature sensor (CHFT) is used to collect temperature and heat flux measurements [1] at the tissue surface. The heat flux is measured with a BF-02 heat flux gauge from Vatell Corp. It produces a voltage signal directly proportional to the heat flux using a nickel-copper differential thermopile between the CHFT chip faces with a calibration factor of 2.1 mV/(W/cm^2). The temperature sensor on the CHFT is a type-K foil thermocouple mounted on the sensor surface next to the tissue. The top face of the CHFT is exposed to a compressed air source which produces cooling from nine air jets exiting from 0.37 mm holes. Figure 1 illustrates the CHFT sitting above the tissue surface under the air jets. The measurement begins with the sensor sitting at thermal equilibrium on the tissue. The thermal event begins when the jets are activated causing a large change in the heat flux. Three CHFT sensors were used to simultaneously collect temperature and heat flux measurements. One of the three sensors was used as a control by attaching it to the unburned surface next to the burns. Amplifiers and a DAQ system were used to collect data with 10 samples per second. Results were averaged for each second. A mathematical model is used to estimate the core temperature, blood perfusion and thermal resistance from the steady state and transient data.
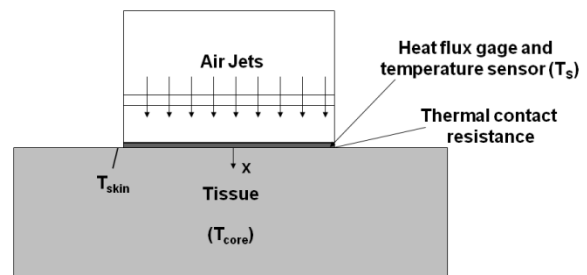

Figure 1. CHFT mounted on the tissue

The Pennes equation [11] is used to model the conduction heat transfer process and the effects of perfusion in the tissue.

$$(\rho c)_t \frac{\partial \theta}{\partial t} = k_t \frac{\partial^2 \theta}{\partial x^2} - (\rho c w)_b \theta \qquad (1)$$

where $\theta(x,t) = T(x,t) - T_{core}$ is the temperature difference between tissue and the entering blood at the core temperature. Subscript b is for blood properties while subscript t represents the tissue properties. The assumption is that ρ, c and k, which are the density, thermal capacity and thermal conductivity of both tissue and blood are assumed to have the same average values k = 0.5 W/m-K, $\rho = 1050$ kg/m^3, and c = 3800 J/kg-K. The blood perfusion is w_b .

The process of developing the analytical solution was described in detail in reference [1]. Temperature measurements at the surface boundary are used as in equation 2, while the boundary in the tissue is specified using equation 3

$$-k \frac{\partial \theta}{\partial x}\Big|_{x=0} = \frac{1}{R''} \left(\theta_S(t) - \theta(0,t) \right) \tag{2}$$

$$\frac{\partial \theta}{\partial x}\Big|_{x \to \infty} = 0 \tag{3}$$

where R'' is the thermal resistance between the sensor and tissue, and the s-subscript stands for the sensor. The complete analytical solution is developed from a combination of the steady-state solution before the thermal event and the transient solution during the thermal event.

The measured sensor temperature profile is modeled as a series of steps, where H(t) is the step function which is defined as

$$H(t - t_n) = \begin{bmatrix} 0, & t < t_n \\ 1, & t \geq t_n \end{bmatrix} \tag{4}$$

where each step corresponds to a temperature in the digital series

$$\theta_S(t) = \theta_S(0) + \sum_{n=1}^{N_{max}} \Delta\theta_{S,n} . H(t - t_n) \tag{5}$$

and $\theta_{S,n}$ represents the steady-state temperature difference between the sensor and core at any n-step, while $\theta_{S,0}$ is before the thermal event is initiated. The solution for the transient heat flux was developed using the Green's function approach.

$$\theta_T(0,t) = \frac{1}{\rho c} \int_{t_0=0}^{t} \frac{1}{R''} \left(\theta_S(t_0) - \theta_{S,0} \right) G(0,t|0,t_0) dt_0 \tag{6}$$

$$q_T = \frac{\theta_T(0,t) - \theta_S(t)}{R''} \tag{7}$$

The Green's function at the surface is

$$G(0,t|0,t_0) = \frac{2 \, e^{-w_b(t-t_0)}}{\sqrt{4\pi\alpha(t-t_0)}} - \frac{erfc\left(\frac{\sqrt{\alpha(t-t_0)}}{k \, R''}\right) e^{\left(\frac{1}{(k \, R'')^2}\alpha - w_b\right)(t-t_0)}}{k \, R''} \tag{8}$$

The initial heat flux was developed using the steady state version of equation 1. The initial heat flux is used to estimate the core temperature in $\boldsymbol{\theta_{S,0}}$ [1].

$$q_i = -k \, \theta_{S,0} \left[\frac{\sqrt{w_b/\alpha}}{1 + R''k \sqrt{w_b/\alpha}} \right] \tag{9}$$

By superposing the initial and transient solutions

$$q_a = q_i + q_T \tag{10}$$

The analytical solution was validated versus 1D finite difference and 2D cylindrical coordinate finite difference solutions [1]. Figure 2 illustrates typical measurements and fit between analytical and measured heat flux. The difference between the sensor and skin temperatures represents the thermal contact resistance between the sensor and skin. The thermal resistance will appear to be higher when burned tissue is present.

Core temperature, thermal resistance, and blood perfusion are the three unknown parameters which are obtained by fitting measured and analytical heat fluxes. The search uses closed predetermined domains for all possible values of both blood perfusion and thermal resistance. The search inside the two domains is done by alternating the search direction and narrowing the search around both domains. Each set of two parameters applied to the initial analytical heat flux with the steady-state solution to evaluate the core temperature. The transient analytical solution is then compared to the measured heat flux during the thermal event. The difference between the measured and analytical values is used to form the average square root of the squared residual. The minimum value of this quantity specifies the best fit and the optimum set of parameters [1].
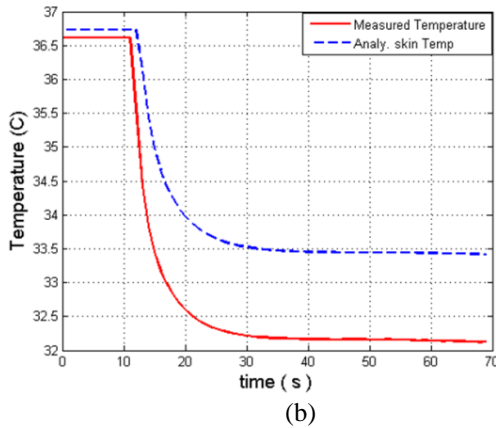

(a)

(b)
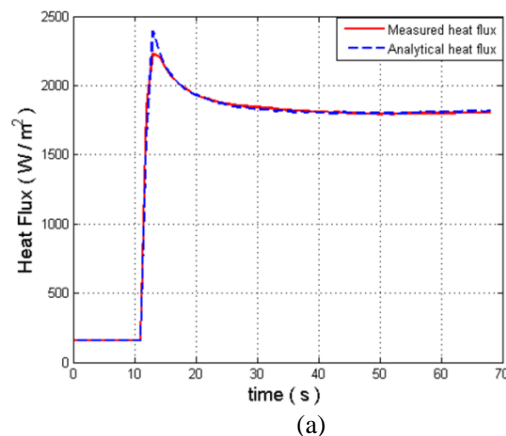
Figure 2. Fitting Analytical and Measured (a) Heat Fluxes (b) Temperatures

IV. QUANTIFYING THE DEGREE OF DAMAGE TO THE TISSUE (DAMAGE FUNCTION)

A finite difference model to calculate temperature distribution, which is resulted from burning the pig tissue using the brass cylinder at 100C^o for each burn time, was created to calculate the penetration depth of damages through tissue for each burn time. A damage function was developed by Moritz and Henriques [4], where thermal damage is approximated using a temperature-dependent rate process, similar to other chemical kinetic processes. An Arrhenius equation is used to quantify this process

$$\frac{d\Omega(x, t_{burn})}{dt} = A \exp\left(-\frac{G}{R\,T(x,t)}\right) \qquad (11)$$

where:

$\Omega(x, t)$ = a damage function

G = an activation energy for the reaction (G = 62,7000 J/mol)

T(x,t) = absolute temperature of a local tissue (calculated from the heat equation at the basal layer)

R = Gas constant (8.36 J/°C/mol)

A = Constant (3.1 × 10^{98} sec^{-1})

The total thermal damage over the time interval from t_o to t_{burn} is

$$\Omega(x, t_{burn}) = \int_{t_0}^{t_{burn}} A\, e^{-G/R\,T(x,t)}\, dt \qquad (12)$$

A finite-difference solution uses an initial temperature of 35°C followed by applying the burn from a cylinder brass at 100°C at the surface which has the averaged estimated values at rest of blood perfusion, thermal resistance and core temperature of, $w_b = 0.003$ ml ml^{-1}s^{-1}, R" = 0.003 m^{2}K/W and $T_{core} = 38$ °C respectively.

The resulting tissue temperature distribution T(x,t_{burn}) from the finite-difference solution for each of the four burns was used to evaluate the damage function from equation 12. The Matlab function Trapz was used to evaluate the integral. A damage function value of 10^4 was used as the criteria for a third degree burn [3]. Figure 3 illustrates the results of the damage function on the Y-axis versus the corresponding depth L$_t$ (mm). It is clear that burn times of 3 and 12 seconds are not a third degree burn. However, burn times of 20 and 75 seconds are third degree burns. The corresponding calculated burn depths for 20 and 75 seconds were L$_{20}$ = 0.14 mm and L$_{75}$ = 1.3 mm repspectively.
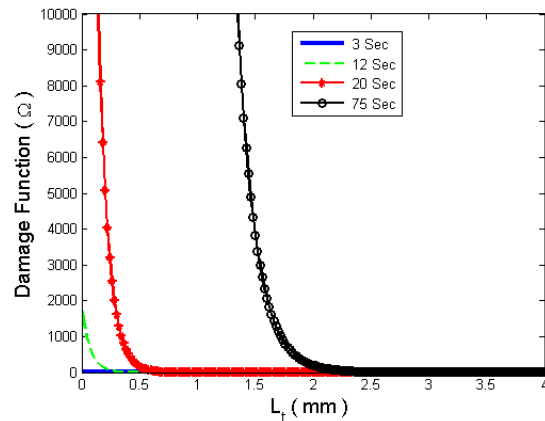

Figure 3. Damage Function Versus Burn Depth

V. RESULTS AND DISCUSSION

A total of 390 tests were collected on the two pigs. One out of every six tests was a control taken on normal tissue beside the burn. After parameter estimation was performed, some of the tests were discarded because one of the estimated values of blood perfusion, thermal contact resistance or core temperature was outside the limits of reasonable values. Usually this was because of a problem in the process of manually placing the probe on the tissue or electrical noise in the data acquisition. A total of 342 tests were used for the final burn evaluations.

Blood perfusion w_b and thermal resistance $R^"$ are the two estimated parameters used to characterize and quantify burn severity. Average of the core temperature was around 38℃. Figure 4 illustrates the average results of blood perfusion (a) and thermal resistance (b) as a function of the implemented burn time (burn severity). Zero burn time represents the control with no burn. The time after the burn is shown as four different symbols and lines, representing one hour, 24 hours, 72 hours and 120 hours after the burn. To demonstrate the deviation of blood perfusion and thermal resistance from the average values, a ninety-five percent confidence interval is shown with each value in the figure. One hour following the burn the blood perfusion has decreased and the thermal resistance has increased for all of the burns except for the lightest, 3 second burn. After 24 hours, however, the

blood perfusion has increased and the thermal resistance has dropped, indicating that the blood is flowing near the surface. The highest blood perfusion is for the 3 second case, showing the strongest inflammation response.
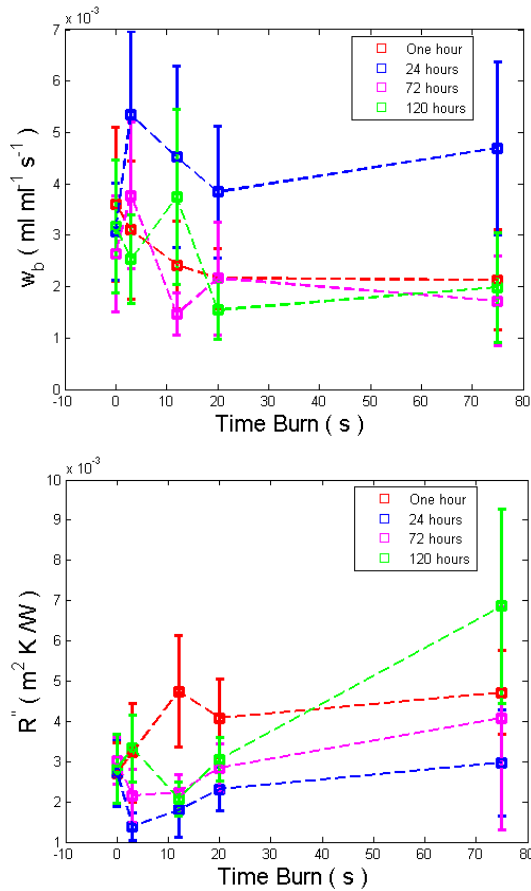
Figure 4. Averaged Values of (a) Blood perfusion and (b) thermal resistance versus burn time

To better visualize the changes with time after the burn, Figure 5 shows only a portion of the results as a function of the time after the burn, with the severity of the burn indicated by three different symbols and lines. Only the values for the undamaged control, 3second burns and 75 second burns are shown. The control value of blood perfusion (a) and thermal resistance (b) remain nearly constant. The blood perfusion increases at 24hours and then decreases. The thermal resistance does theopposite. The blood perfusion values for the 75 second burn are always less than the 3 second burn, while the thermal resistance values are always higher for the 75 second burn. The trends are clear. After 120 hours the 3 second burn is within the uncertainty of the control tissue (no burn). As would be expected of tissue with a layer of dead material on top, the 75 second burn has lower blood

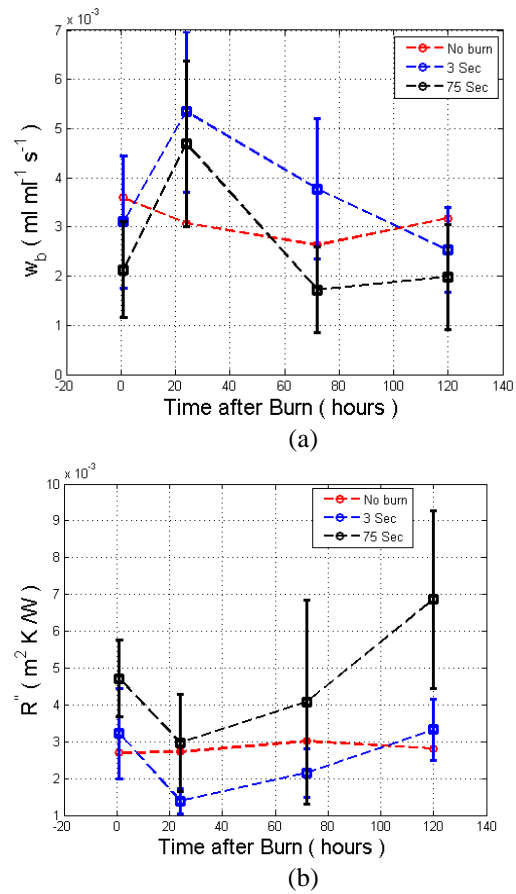perfusion   and   higher   thermal   resistance.

Figure 5. Averaged Values of (a) Blood Berfusion and (b) Thermal Resistance versus Time fter Burn

The thermal resistance is in general composed of two resistances in series. The first is the contact resistance between the CHFT sensor and the surface of the tissue, $R_0^{"}$. The second is the resistance of a non-perfused layer, L/k, where L is the tissue thickness and k is the tissue thermal conductivity [2].

$$R^{"}(L) = R_0^{"} + \frac{L}{k} \qquad (13)$$

If it is assumed that severely burned tissue does not have any perfusion, measurements of the thermal resistance can be used to estimate the thickness of this layer.

$$L = k * \left(R^{"} - R_0^{"}\right) \qquad (14)$$

A previous study [2] has shown the validity of this approach using plastic layers to simulate non-perfused tissue. The perfusion and thermal resistance sensor was successfully used to estimate the thickness of the non-perfused layer based on the thermal measurements with the CHFT. The value of $R_0^{"}$ is assumed to be equal to the thermal resistance for the healthy control tissue. The thickness of the burned tissue can then be estimated from equation 15 using the corresponding thermal resistance values for that tissue as a function of time after the burn.

Figure 6 illustrates the estimated burn depth from thermal measurements using the averaged thermal resistance. The burn times have been converted to the corresponding depth causing third degree burn $\Omega = 10^4$ from Figure 3. Each thickness is plotted on a separate axis. Notice, there are no corresponding depth for burn times of 3 and 12 seconds, because there is no third degree burn. The predicted thickness is between that measured thermally at 72 and 120 hours.
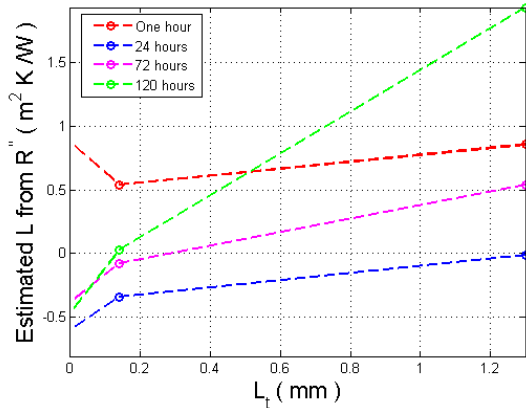

Figure 6. Estimated Burn Depth at Each Monitored Time

To combine the effects shown by changes in both the blood perfusion and the thermal resistance, the burn factor is introduced to better describe the simultaneous changes in both variables

$$ BF = \left[\frac{w_{b,0}}{w_{b,burn}} \right] \times \left[\frac{R_{burn}^{"}}{R_0^{"}} \right] \tag{15} $$

where $w_{b,0}$ is the local blood perfusion of a healthy tissue with no burn imposed, $w_{b,burn}$ is the local blood perfusion of the burned tissue, $R_0^{"}$ is the local thermal resistance of a healthy tissue with no burn imposed, and $R_{burn}^{"}$ is the local thermal resistance of the burned tissue. Because the blood perfusion for burned tissue decreases and the apparent thermal resistance increases as shown in Figures 4 and 5, the values change in opposite directions. The burn factor therefore uses the inverse of the blood perfusion ratio, which combines these effects to increase for burned tissue.

Figure 7 shows the calculated values of the burn factor. It is plotted versus the burn times in Figure 7a and versus the time after burn in Figure 7b. The signal for the 20s and 75s burns is very strong at the 1 hour and 120 hour times after burn. It appears that there is a healing response of the tissue at 24 hours post burn for all of the burn severities. The 20s and 75s burns then become progressively worse, indicating that they are not healing. Therefore, burn factor *BF* appears to be a good indicator of the direction of the tissue response. Notice that for any reversible damage, there will be not a large effect of the thermal resistance and the ratio of blood perfusion will reflect the activation of the inflammatory system to pump more blood to the tissue. Conversely, with severe burns the blood perfusion ratio will be deactivated and the

thermal resistance ratio increases. The 12s burn as seen in Fig. 7b does not have a clear signal and may actually be healing at longer times. Burn times below 20 seconds have values of burn factor closer to one with some deviation related to responses to the inflammatory system.
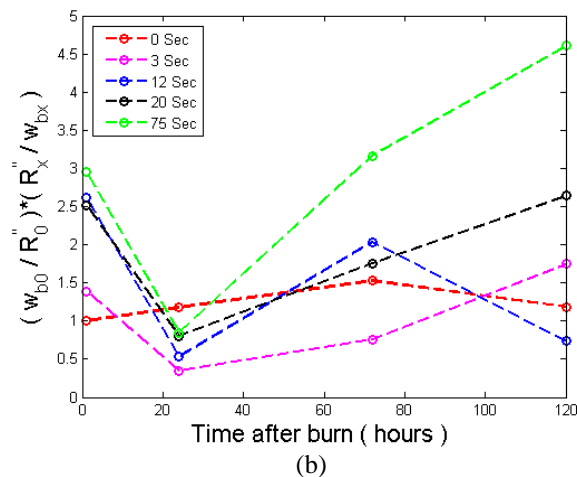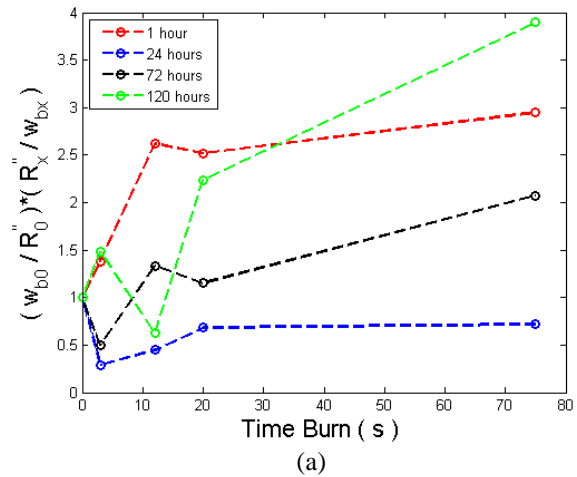

(a)

(b)

Figure 7. Burn Factor for Different (a) Burn Times and (b) Time fter Burn

To further illustrate the value of the burn factor, it was applied to a set of experiments applying a simulation of burns using a phantom tissue system. Dead tissue was simulated with a layer of plastic over a perfused porous media simulating healthy tissue. Three different flow rates were used for the perfusion and a range of plastic thicknesses. The results are shown in Figure 8 with the burn factor as a function of the layer thickness for the three flow rates. The flow rate has little influence on the results, but the burn factor shows a strong function of the layer thickness. Values are comparable to those in this paper for the pig burns. The thickness values are smaller, but the thermal conductivity of the plastic is about one-half that of tissue. In addition, there is a sharp demarcation from the plastic layer with zero perfusion to the fully perfusion phantom tissue. In real tissue there would not be such a sharp demarcation.
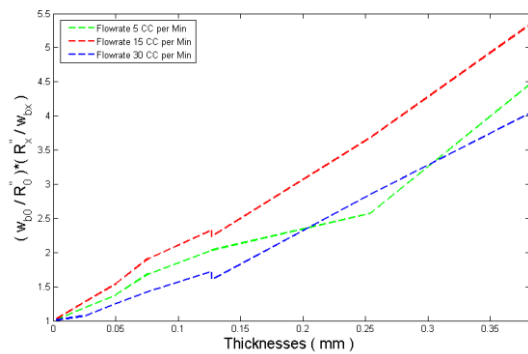
Figure 8. Burn Factor Applied to Phantom Tissue Experiments

VI. CONCLUSIONS

The pig experiment burn results support the ability of the new perfusion-thermal resistance system to predict burn depth from thermal measurements. Four different burn times were implemented on the animal skin to give a range of burn severity. Results illustrate the ability of the method to quantify burns at each implemented burn time, using averaged estimated values of thermal resistance and blood perfusion. Burn depths were quantified from the thermal resistance measurements on healthy and burned tissue. The values gave a reasonable match with the predicted burn depths from estimates of the damage factor and laboratory measured thicknesses of 20 and 75 burn times from the surgeon with values of 0.3 mm and 2 mm, respectively. The surgery was done without shaving the pig's hair, which might explain why the control value of thermal resistance was slightly higher than human values. The burn factor was introduced as a more sensitive quantitative indicator of the tissue damage and healing responses. Values of the burn factor showed that the model is sensitive to the different burn severity and the corresponding inflammatory responses.

REFERENCES

[1] Alkhwaji, A., Vick, B., and Diller, T., "*New mathematical model to estimate tissue blood perfusion, thermal contact resistance and core temperature*," Journal of Biomechanical Engineering, Vol.134, 2012, 081004, pp. 1-8.

[2] Abdusalam Alkhwaji, Brian Vick, Tom Diller, "*Modelling and Estimating Simulated Burn Depth Using the Perfusion and Thermal Resistance Probe*," Journal of Medical Device, Vol.7, September 2013, 031003, pp. 1-9.

[3] Diller, K.R., Modeling of Bioheat Transfer Processes at High and Low Temperatures, Advances in Heat Transfer 22, 1992, 157-357.

[4] Moritz, A. R., Henriques F. C., Jr., "*Studies of thermal injury: (II). The relative importance of time and surface temperature in the causation of cutaneous burns.*" American Journal of Pathology, 1947, 23: 695-720.

[5] Jaskille, A. D., Shupp, J., Jordan, M., and Jeng, J. C., "*Critical Review of Burn depth Assessment Techniques: Part I. Historical Review,*" 2009, *Journal of Burn Care & Research*, Vol. 30, pp. 937-947.

[6] Renkelska, A., Nowakowski, A., Kaczmarek, M., and Ruminski, J., 2006, "*Burn Depths Evaluation Based on Active Dynamic IR Thermal Imaging – A Preliminary Study,*" *Burns*, Vol. 32, pp. 867-878.

[7] Mileski, W. J. L. Atiles, G. Purdue, R. Kagan, J. R. Saffle, D. N. Herndon, D. Heimbach, A. Luterman, R. Yurt, C. Goodwin, J. L. Hunt, 2003, "*Serial Measurements Increase the Accuracy of Laser Doppler Assessment of Burn Wounds,*" *Journal of Burn Care & Rehabilitation*, Vol. 24, pp. 187-191.

[8] Jeng, J. C., Bridgeman, A., Shivnan, L, Thornton, P., Alam, H., Clarke, T., Jablonski, K., and Jordan, M., 2003, "*Laser Doppler Imaging Determines Need for Excision and Grafting in Advance of Clinical Judgment: A Prospective Blinded Trial,*" *Burns*, Vol. 29, pp. 665-670.

[9] Stewart, C. J., R. Frank, K.R. Forrester, J. Tulip, R. Lindsay, R.C. Bray, 2005, "*A comparison of two laser-based methods for determination of burn scar perfusion: Laser Doppler versus laser speckle imaging." Journal of Burns,* Vol. 31, pp. 744-752.

[10] Jaskille, A. D., Ramella-Roman, J., Shupp, J., Jordan, M., and Jeng, J. C., "*Critical Review of Burn Depth Assessment Techniques: Part II. Review of Laser Doppler Technology,*" 20010, Vol. 31, pp. 151-157.

[11] Pennes, H. H., 1948, "*Analysis of Tissue and Arterial Blood Temperatures in the Resting Human Forearm,*" *J. Appl. Physiol.*, Vol. 1, pp. 93-122.

[12] Vajkoczy, P., H. Roth, P. Horn, T. Lucke, C. Taumé, U. Hubner, G.T. Martin, C. Zappletal, E. Klar, L. Schilling, P. Schmiedek, 2000, "*Continuous Monitoring of Regional Cerebral Blood Flow: Experimental and Clinical Validation of a Novel Thermal Diffusion Microprobe,*" *Journal of Neurosurgery,*" Vol. 93, pp. 265-274.

[13] Khot. M. B., P. K. M. Maitz, B. R. Phillips, H. F. Bowman, J. J. Pribaz, D. P. Orgill, 2005, "*Thermal Diffusion Probe Analysis of Perfusion Changes in Vascular Occlusions of Rabbit Pedicle Flaps,*" *Plastic Reconstructive Surgery.,* Vol. 115, No. 4, pp. 1103-1109.

[14] Maitz, Peter K. M, M. B. Khot, H. F. Mayer, G. T. Martin, J. J. Pribaz, H. F. Bowman, D. P. Orgill, 2005, "Continuous and Real-Time Blood Perfusion Monitoring in Prefabricated Flaps," Journal of Reconstructive Microsurgery. Vol. 20, No. 1, pp. 35-41.

[15] Ricketts, P. L., Mudaliar, A. V., Ellis, B. E., Pullins, C. A., Meyers, L. A., Lanz, O. I., Scott, E. P., and Diller, T. E., 2008, "Non-Invasive Blood Perfusion Measurements Using a Combined Temperature and Heat Flux Probe," *International Journal of Heat and Mass Transfer*, Vol. 51, pp. 5740-5748.

[16] Mudaliar, A. V., Ellis, B. E., Ricketts, P. L., Lanz, O. I., Scott, E. P., and Diller, T. E., 2008, "*A Phantom Tissue System for the Calibration of Perfusion Measurements,*" *ASME Journal of Biomechanical Engineering*, Vol. 130, No. 051002.

[17] Mudaliar, A. V., Ellis, B. E., Ricketts, P. L., Lanz, O. I., Lee, C. Y., Diller, T. E., and Scott, E. P., 2008, "*Non-invasive Blood Perfusion Measurements of an Isolated Rat Liver and Anesthetized Rat Kidney,*" *ASME Journal of Biomechanical Engineering*, Vol. 130, No. 061013.

[18] Jacquot, A., Lenoir, B., Dauscher, A., Stölzer, M., and Meusel J., "*Numerical simulation of the 3w method for measuring the thermal conductivity,*" Journal of Applied Physics, Vol. 91, 2002, pp. 4733-38.

[19] Muhammad Javed, Kayvan Shokrollahi, "*VACUETTE for burn depth assessment – A simple and novel alternative use for a ubiquitous phlebotomy device,*" Burns, 38, 2012, 1084-1085

[20] J. M. Still, E.J. Law, K. G. Klavuhn, T.C. Island, J. Z. Holtz, "*Diagnosis of burn depth using laser-induced indocyanine green fluorescence: a preliminary clinical trial,*" Burns, 27, 2001, 364-371.

[21] Khanh Nguyen, Diane Ward, Lawrence Lam, Andrew J. A. Holland*, "Laser Doppler Imaging prediction of burn wound outcome in children: Is it possible before 48 h?,"* Burns, 36, 2010, 793-798

BIOGRAPHIES

Thomas Diller He received Bsc degree in Mechanical Engineering from Carnegie-Mellon University, in 1972. He got Msc degree in Mechanical Engineering from Massachusetts Institute of Technology / USA in 1974. Moreover, he got Sc.D. degree in Mechanical Engineering from Massachusetts Institute of Technology/USA in 1977. He is currently professor in Department of Mechanical Engineering at Virginia Tech University / USA. His research field is heat flux sensor development and calibration, turbulent heat transfer, and biomedical thermal instrumentation.

Abdusalam Imhmed k. Al khwaji was born in Zliten /Libya, on August 23, 1972. He received Bsc degree in Mechanical Engineering from Omar Almukthar University, in 1996. He got Msc degree in Mechanical Engineering (CSE) from Technical University of Braunschweig /Germany in 2006. Moreover, he got PhD degree in Mechanical Engineering & option in Biomedical Engineering from Virginia Tech University/USA in 2013. He is currently lecturer in Department of Mechanical Engineering at AL Asmarya Islamic University/Libya. His research field is computational & experimental heat transfer, biomedical thermal instrumentation, robot control.